This article is part of the

Proceedings of the 16th Minisymposium Verfahrenstechnik and 7th Partikelforum (TU Wien, Sept. 21/22, 2020)

Title:
The porosity of iron ore sinter

Corresponding author:
Christof Lanzerstorfer (FH OOE), c.lanzerstorfer@fh-wels.at

Date of submission:
25.02.20

Date of revision:
25.08.20

Date of acceptance:
27.08.20

Chapter ID:
MoP3-(12)

Length:
4 pages

Download available from (online, open-access):
http://www.chemical-engineering.at/minisymposium

ISBN (full book):
978-3-903337-01-5

Porosity of iron ore sinter

Daniel Lampl[1], Christof Lanzerstorfer[1,*]
1: School of Engineering, University of Applied Sciences Upper Austria, Austria
* Corresponding author: c.lanzerstorfer@fh-wels.at

Keywords: ironmaking, iron ore sinter, porosity, size dependence

Abstract

Iron ore sinter is the main iron-bearing charge in many blast furnaces for ironmaking. A certain porosity of the charge is required to allow the flow of the carbon monoxide-rich reduction gas. The porosity of an accumulation of porous particles is of two types: the interparticle porosity resulting from the voids in the bulk and the intraparticle porosity of the porous particles. In this study the different porosities for sinter were determined using simple methods: measurement of the skeleton density by liquid pycnometry, measurement of the bulk density and determination of the envelope volume of the particles. The average skeleton density of the investigated sinter particles was 4.38 ± 0.22 g/cm³ and the average intraparticle porosity was 0.216 ± 0.037. For both parameters no distinct size dependence was observed.

Introduction

In integrated steel mills the process of ironmaking usually involves two main process units, the sinter plant and the blast furnace (BF). In the sinter plant iron ore fines are agglomerated together with fluxes and iron-rich in-plant return fines to sinter. In the BF the iron oxides of the ore are reduced to metallic iron [1,2]. The BF is charged continuously from the top of the furnace in layers of iron-bearing materials (sinter, pellets, etc.) and coke. The charge flows slowly downwards in the furnace shaft where it is in contact with a countercurrent flow of hot, carbon monoxide-rich combustion gases produced from the hot blast injected via tuyeres by reaction with the coke. This carbon monoxide reduces the oxides. To enable the upwards gas flow voids between the particles of the charge are required. These voids can be characterized by the porosity of the bulk.

The porosity ε of a solid bulk material is defined as the ratio of the volume of the accessible pores and voids V_P to the bulk volume occupied by the solid V_B [3].

$$\varepsilon = \frac{V_p}{V_B} = 1 - \frac{V_S}{V_B} \quad (1).$$

For non-porous particles the porosity can be obtained from the mass m_S and the volume of the bulk together with the material density ρ. For porous particles the skeleton density ρ_{Sk} has to be used, which includes closed pores in the particle volume.

$$\varepsilon = 1 - \frac{m_S / \rho_{Sk}}{V_B} \quad (2).$$

In dry bulk solids where the pores and voids are filled with air the mass of the solids is nearly identical with the mass of the bulk. In this case the porosity can be calculated with Equation (3):

$$\varepsilon = 1 - \frac{\rho_B}{\rho_{Sk}} \quad (3).$$

For porous particles the porosity consists of two types: the interparticle porosity ε_e and the intraparticle porosity ε_i. The interparticle porosity is the ratio of the volume of void space between the individual particles to the bulk volume of the particles, while the intraparticle porosity is the ratio of the volume of open pores inside the individual particles to the bulk volume occupied by the solid [3]. Equation (4) shows how the interparticle porosity and the intraparticle porosity make up the total porosity:

$$\varepsilon = \varepsilon_e + (1 - \varepsilon_e) \cdot \varepsilon_i \quad (4).$$

For the gas flow through the bed of sinter particles and the resulting pressure drop the interparticle porosity is the more important type of porosity since the velocity of the gas flow in pores is quite low. In contrast, for reduction of the iron oxide the intraparticle porosity is important for the transport of carbon monoxide.

The intraparticle porosity of particles can be measured by mercury porosimetry or by gas adsorption. However, these methods are quite cumbersome. An easier way to determine the intraparticle porosity of a particle is from its envelope volume V_E, which is defined as the total volume of the particle, including closed and open pores.

$$\varepsilon_i = 1 - \frac{m_S / \rho_{Sk}}{V_E} \quad (5).$$

The required skeleton density can be measured by gas pycnometry or liquid pycnometry using Archimedes' Principle [4]. In liquid pycnometry using a displacement liquid with the density ρ_L, the skeleton density is obtained with Equation (6):

$$\rho_S = \frac{m_S}{V_E - \frac{m_{tot} - m_{pyc} - m_S}{\rho_L}} \quad (6),$$

where m_{tot} is the total mass of the pycnometer including the particle and the liquid filling, while m_{pyc} is the mass of the empty pycnometer and m_S is the mass of the particle.

The interparticle porosity can be calculated from the intraparticle porosity and the total porosity using Equation (7):

$$\varepsilon_e = \frac{\varepsilon - \varepsilon_i}{1 - \varepsilon_i} \quad (7).$$

The aim of this study was to determine the skeleton density, the interparticle porosity and the intraparticle porosity of iron ore sinter particles from an industrial sinter plant.

Materials and methods

Sinter particles

Iron ore sinter material was obtained from an industrial sinter plant for sinter cooling experiments. Several particles with different particles size were selected randomly for the investigation. The bulk density of the sinter material was

determined by pouring sinter into a vessel with a defined volume and subsequently measuring the mass of the sinter material was 1890 kg/m³. The average size of the sinter used in the BF varies slightly from plant to plant. However, the size range of sinter particles is typically from 5 -50 mm.

Table 1 gives an overview of the investigated sinter particles and Figure 1 shows some examples of particles.

Table 1. Sinter materials used in the tests

Sample	Mass in g	Equivalent diameter in mm
S1	130.3	45
S2	82.18	38
S3	59.04	32
S4	56.45	31
S5	46.38	30
S6	43.09	28
S7	37.29	27
S8	35.37	26
S9	28.09	26
S10	29.23	25
S11	28.39	25
S12	27.05	25
S13	26.91	24
S14	21.47	23
S15	19.12	22
S16	16.27	21
S17	15.45	21
S18	13.32	19
S19	6.90	16
S20	2.89	12

Figure 1. Iron ore sinter particles investigated

For the particles where the envelope volume was determined the equivalent diameter was calculated from it. For the other particles the equivalent diameter was estimated from their overall dimensions.

Envelope volume

The envelope volume of the sinter particles was measured with a GeoPyk 1360 envelope density analyzer from Micromeritices. In such measurements the sinter particles are packed into a bed of DryFlo© powder, which has a certain bulk density under the prevailing packing conditions. The particle size range of the powder specified by the manufacture is 30-300 µm.

Skeleton density

The skeleton density of the sinter particles was determined by liquid pycnometry where n-heptane with a density of 0,6812 g cm^{-3} at 20°C was used as displacement liquid. Figure 2 shows one of the used pycnometers.

Figure 2. Liquid pycnometer for larger particles

Results

The results of the measurements are summarized in Table 2. The average value of the skeleton density was 4.38 ± 0.22 g/cm³. The variation of the skeleton density might partly be caused by variations in the chemical composition of the sinter particles and partly by a varying fraction of closed pores which are not interconnected with other pores and hence not accessible.

Figure 3 shows the size dependence of the skeleton density. No distinct size-dependence was observed.

The average intraparticle porosity of the investigated sinter particles was 0.216 ± 0.037. The reason for the variation of the intraparticle porosity is the varying fraction of pores in different sinter particles.

A porosity of the bulk of sinter particles of 0.57 results when the average skeleton density is used. This compares well with reported values of the porosity of iron ore sinter in the range of 0.52 to 0.58 [5-7].

Table 2. Sinter materials used in the tests

Sample	Skeleton density in g/cm³	Envelope volume in cm³	Intraparticle porosity
S1	4.43 ± 0.06	-	-
S2	4.21 ± 0.03	-	-
S3	4.12 ± 0.05	17.39	0.176
S4	4.44 ± 0.03	15.96	0.203
S5	4.36 ± 0.03	13.64	0.220
S6	4.48 ± 0.02	11.94	0.195
S7	4.43 ± 0.00	10.73	0.216
S8	4.10 ± 0.10	-	-
S9	4.22 ± 0.14	8.74	0.239
S10	4.69 ± 0.00	8.00	0.221
S11	4.19 ± 0.09	-	-
S12	4.49 ± 0.04	8.39	0.282
S13	4.16 ± 0.05	-	-
S14	4.72 ± 0.09	6.06	0.249
S15	4.30 ± 0.15	5.68	0.216
S16	4.52 ± 0.52	-	
S17	4.37 ± 0.00	4.66	0.241
S18	4.68 ± 0.10	-	-
S19	4.64 ± 0.23	-	-
S20	3.99 ± 0.06	0.84	0.137
Average	4.38 ± 0.22		0.216 ± 0.037

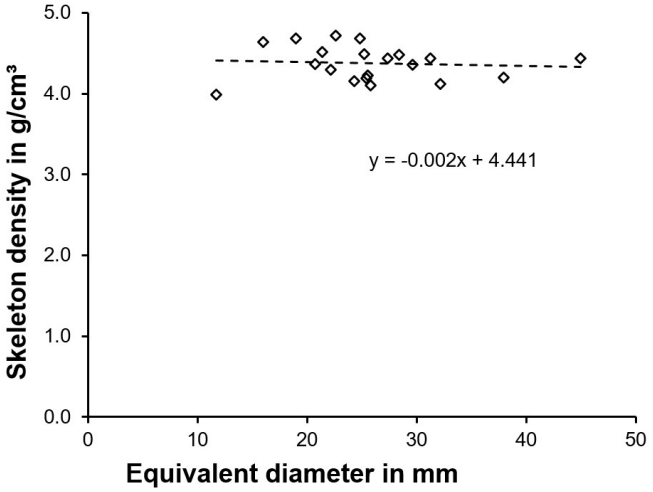

Figure 3. Size dependence of the skeleton density of sinter particles

Figure 4 shows the size dependence of the intraparticle porosity. No distinct size-dependence was observed.

Using the average intraparticle porosity the resulting interparticle porosity of the investigated sinter material according to Equation (7) is 0.45.

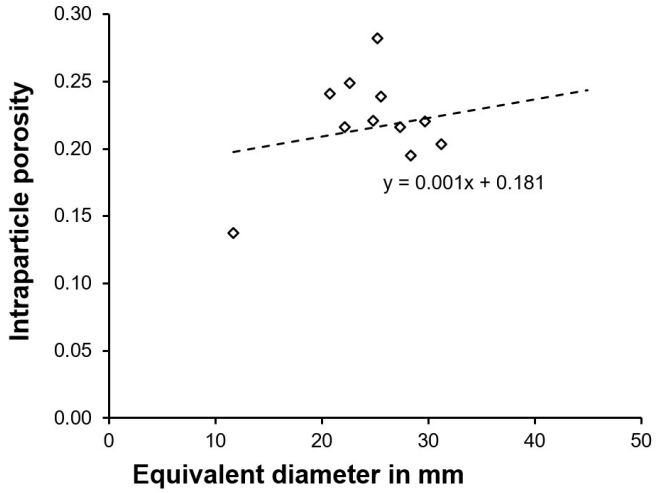

Figure 4. Size dependence of the intraparticle porosity

Conclusions

The applied method is a simple procedure for the determination of the intraparticle porosity in comparison with mercury porosimetry or by gas adsorption methods.

From the experiments the following conclusions can be drawn:

- the average skeleton density of the investigated sinter particles was 4.38 ± 0.22 g/cm³. With a relative standard deviation of 5% the variation of the value was not very great.
- no distinct size dependence of the skeleton density was observed.
- the average intraparticle porosity of the investigated sinter particles was 0.216 ± 0.037. The relative standard deviation was 17%.
- no distinct size dependence of the intraparticle porosity was observed.

Acknowledgement

The determination of the envelope volume by A. Böhm (Montanuniverität Leoben) and proofreading by P. Orgill are gratefully acknowledged. The study was financially supported by K1-MET. K1-MET is a member of COMET – Competence Centers for Excellent Technologies and is financially supported by the BMVIT (Federal Ministry for Transport, Innovation and Technology), BMWFJ (Federal Ministry of Economy, Family and Youth), the federal states of Upper Austria, Styria and Tyrol, SFG and Tiroler Zukunftsstiftung. COMET is managed by FFG (Austrian research promotion agency).

References

[1] Peacey, J.G., and Davenport, W.G., The Iron Blast Furnace Theory and Practice. Elmsford: Pergamon Press, 1979.

[2] Geerdes, M., Chaigneau, R., Kurunov, I., Lingiardi, O., and Ricketts, J., Modern Blast Furnace Ironmaking – an introduction. 3rd Edition. Amsterdam: Delft University Press, 2015.

[3] ISO 15901-1:2016. Evaluation of pore size distribution and porosity of solid materials by mercury porosimetry and gas adsorption — Part 1: Mercury porosimetry, 2016.

[4] ASTM B962-17, Standard Test Methods for Density of Compacted or Sintered Powder Metallurgy (PM) Products Using Archimedes' Principle, ASTM International, West Conshohocken, PA, 2017.

[5] Liu, Y., Wang, J., Cheng, Z., Yang, J., and Wang, Q., "Experimental investigation of fluid flow and heat transfer in a randomly packed bed of sinter particles," International journal of heat and mass transfer, vol. 99,

pp. 589-598, 2016.

[6] Tian, F.-Y., Huang, L.-F, Fan, L.-W., Qian, H.-L., Gu, J.-X., Yu, Z.-T., Hu, Y.-C., Ge, J., and Cen, K.-F., “Pressure drop in a packed bed with sintered ore particles as applied to sinter coolers with a novel vertically arranged design for waste heat recovery,” Journal of Zhejiang University – SCIENCE A, vol. 17, no. 2, pp. 89-100, 2016.

[7] Yin, J., Lv, X., Bai, C., and Qiu, G., Numeric simulation of the cooling process of the iron ore sinter. In: Hwang, J.-Y., Drelich, J., Downey, J., Jiang, T., and Cooksey, M., (Eds.), 2nd International Symposium on High-Temperature Metallurgical Processing. Hoboken: John Wiley & Sons, pp. 403-410, 2011.